Research Article | Vol. 30, No. 3 / 31 Jan 2022 / Optics Express 3329
Optics EXPRESS

Efficient high-energy Raman soliton generation in a Tm:doped large mode area fiber amplifier

ROLAND A. RICHTER,[1,*] NIKOLAI TOLSTIK,[1,2] AND IRINA T. SOROKINA[1,2]

[1]Department of Physics, NTNU, Norwegian University of Science and Technology, Trondheim, Norway
[2]ATLA Lasers AS, Trondheim, Norway
[*]roland.richter@ntnu.no

Abstract: We report the Tm-doped all-fiber MOPA based on a LMA active fiber generating Raman solitons tunable in the range 1970-2300 nm directly from the LMA fiber. By tuning the chirp of the input pulse we reached more than 90 % energy transfer efficiency to Raman soliton. Solitons with 125 fs duration and up to 24 nJ energy are demonstrated in LMA fiber amplifier. We show experimentally that Raman solitons experience both amplification and absorption in active fiber components of the laser system and that the energy of a Raman soliton generated in an LMA fiber amplifier is limited by the soliton area theorem.

1. Introduction & state of the art

High-power and -energy tunable ultrashort pulsed fiber laser sources operating above 2000 nm gain more and more interest due to the large range of possible applications, such as eye-safe LIDAR, multi-photon microscopy, optical coherence tomography, spectroscopy as well as marking and micro-machining, to name a few. The spectral window between 2000 nm and 2500 nm is of special interest due to the transparency of the atmosphere around 2100-2200 nm as well as presence around 2300-2500 nm of several molecular absorption lines enabling, for example, differential absorption spectroscopy. Even though thulium-doped silica based fibers typically support amplification in the range of 1800-2050 nm [1] and do not cover the whole range up to 2500 nm, it has been demonstrated that it is possible to generate pulses at up to 2500 nm directly from the Tm fiber amplifiers by using Raman self-frequency pulse conversion to either shift the central wavelength of the pulse or broaden the pulse sufficiently enough to fully cover the targeted spectrum [2–4].

Ultrashort-pulse tunable Raman soliton-based Tm-doped fiber amplifiers have been demonstrated by several research groups in silica fibers [5–11]. These papers report tuning performance with soliton central wavelengths ranging from 1950 nm to 2500 nm, and pulse durations of 100-200 fs. Energy transfer efficiency to Raman soliton (ratio of the Raman soliton energy to the total output energy) is typically 40-60 %. Several approaches have been proposed to raise the transfer efficiency over 90 % [9,11]. When it comes to the energy of the solitons the published results vary, with some papers reporting Raman soliton energies over 10 nJ [7,9], while others insisting that the Raman soliton in the single mode silica fiber is limited at the energy level of a few nJ [12,13].

In order to elucidate the reason for such spread of reported values and to find the way to precisely control both, the amount of Raman frequency shift as well as the pulse energy, we carry out a careful theoretical and experimental analysis here. Indeed, the fiber amplifier is seeded by an ultrashort pulse ($T_0 <$ ps) which is generated as fundamental optical soliton in a femtosecond fiber oscillator, but weakened to $< 10\%$ of its original energy after leaving the oscillator through the output coupler. Such a pulse will experience dispersive broadening and acquire chirp while being transmitted through the passive fiber on the way towards the fiber amplifier. The amount of chirp acquired by the seed pulse is an important parameter, which defines one of the different operation

#446612 https://doi.org/10.1364/OE.446612
Journal © 2022 Received 21 Oct 2021; accepted 28 Nov 2021; published 18 Jan 2022

Optics EXPRESS

regimes of the amplifier. If the chirp value is high enough to reduce nonlinear optical effects during the amplification sufficiently to minimize pulse shape modifications (i.e. the nonlinear length is approximately equal to the dispersive length), then the laser system can be described as a chirped pulse amplifier [14–16]. If the chirp value is not as high, then the nonlinear effects will be strong in the amplifier fiber, and we will end up with a system generating, in general case, a broadband "white light" supercontinuum, formed out of red-shifted Raman solitons [17,18]. However, there is a narrow range of parameters, where the pulse can be recompressed into a fundamental soliton while being transmitted through the amplifier fiber.

G. P. Agrawal has described the process of Raman soliton formation in a passive fiber with anomalous dispersion [19]. He showed that soliton formation in such a fiber is possible, if the pulse is pre-chirped positively (for example, by transmitting through the normal dispersion fiber), that the value of the chirp will affect the amount of the energy lost during the soliton stabilization process, and finally will define the efficiency of the energy transfer to a soliton. It was also shown that the pulse can this way be recompressed to a shorter soliton, and that the compression factor both for a sech-shaped soliton [19] and Gaussian-shaped pulse [20] can be calculated as:

$$\frac{T_1}{T_0} = \sqrt{\left(1 + \frac{C\beta_2 z}{T_0^2}\right)^2 + \left(\frac{\beta_2 z}{T_0^2}\right)^2}, \tag{1}$$

with T_1 the pulse duration after propagation and T_0 the initial pulse duration. C describes the chirp parameter, β_2 the dispersion of the fiber and z the propagated distance.

The chirp parameter C of the pulse can be calculated as

$$C = \frac{z}{L_D} = \frac{z|\beta_2|}{T_0^2} = \frac{\mathrm{GDD}}{T_0^2}, \text{[19]}. \tag{2}$$

Agrawal et al. limited their modelling to the case of soliton formation in passive fibers. In active fiber, i.e. inside the fiber amplifier, the pulse energy increases, self-phase modulation is way stronger, and thus the pulse can be recompressed to a shorter soliton also in the case of negative pulse chirp.

The energy of the fundamental soliton is limited by properties of the fiber, and can be calculated using the soliton area theorem [19,21]:

$$E_p = \frac{2|\beta_2}{|\gamma T_0}, T_0 = \frac{2|\beta_2|}{|\gamma|E_p} \tag{3}$$

with β_2 the group velocity dispersion (GVD) in the fiber, γ the nonlinear parameter of the fiber (given by Eq. (4)) and T_0 the pulse duration (defined via $T_0 = T_{\mathrm{FWHM}}/1.7626$ for sech^2-pulses). The nonlinear parameter is defined as

$$\gamma(\omega_0) = \frac{n_2(\omega_0)\omega_0}{cA_{\mathrm{eff}}} \tag{4}$$

with A_{eff} the effective mode area and n_2 the wavelength-dependent nonlinear refractive index of the fiber.

For example, for the case of 130 fs pulses at 2 µm wavelength in standard telecom silica fibers ($T_0 = \frac{130\mathrm{fs}}{1.7626}$, $\beta_2 \approx -1.43 \times 10^{-25}\mathrm{s}^2\mathrm{m}^{-1}$ [22], $A_{\mathrm{eff}} = 100\,\mu\mathrm{m}^2$ and $n_2 = 2.5 \times 10^{-20}\mathrm{m}^2\mathrm{W}^{-1}$) we obtain the following soliton energy limit:

$$E_p = \frac{2|\beta_2}{|\gamma T_0} = 5.4\,\mathrm{nJ} \text{ with } \gamma = \frac{n_2 \cdot 2\pi}{\lambda A_{\mathrm{eff}}} = 714 \times 10^{-6}\mathrm{m}^{-1}\mathrm{W} \tag{5}$$

If the spectrum of the soliton transmitted through the fiber is broad enough and the energy is high enough, it will experience the so-called Raman-induced self-frequency shift (RIFS) [21] or

Optics EXPRESS

intra-pulse Raman scattering, where its central wavelength is shifted towards the red wavelengths while propagating through the fiber. A soliton which experiences such a shift is called "Raman soliton". This frequency shift $\Omega(z)$ in [Hz] depends on the distance z the soliton travels through the fiber, and can be calculated as

$$\Omega(z) = -\frac{8T_R|\beta_2|}{15T_0^4}z \tag{6}$$

with β_2 the dispersion value of the fiber in $\left[\mathrm{fs}^2\mathrm{m}^{-1}\right]$, $T_R \approx 3$ fs according to Agrawal et al. [19]. Eq. (6) is valid for pulses, where the chirp is negligibly small and does not change while the pulse propagates through the fiber, i.e. for soliton pulses. From Eq. (3) it follows that $T_0 \propto E_p^{-1}$ and the dependence of the frequency shift on the soliton energy and -wavelength can be given as:

$$\Omega(z) = -\frac{8T_R}{15|\beta_2|^3}\frac{\pi^4 n_2^4}{\lambda^4 A_{\mathrm{eff}}^4}E_p^4 z. \tag{7}$$

This confirms that

$$\Omega(z) \propto E_p^4, \tag{8}$$

i.e. there is a strong dependence of the Raman self-frequency shift on the pulse energy.

The dependence of the parameters of Raman-induced self-frequency shift process on both the chirp acquired by the femtosecond pulse and the energy of the soliton formed in the fiber amplifier show that precise control of both is necessary for stable and efficient operation of the Raman soliton amplifier.

As shown above, the energy of a soliton formed in a fiber amplifier depends on the effective mode area of the amplifier fiber. Getting back to the example above, increasing the effective mode diameter from 10 µm (standard telecom fiber) to 25 µm (large mode area fiber) would increase the theoretical soliton energy limit from 5 nJ to 34 nJ. This approach was tested experimentally for Er-doped fiber amplifier around 1500 nm [23]. In a very large mode area (VLMA)-based Er-doped fiber amplifier (fiber core diameter of 50 µm) the solitons with an energy of 21 nJ at 1650 nm and a duration of 86 fs were obtained, while the amplifier was seeded with 600 fs-chirped pulses at 1560 nm and pumped by a continuous wave (CW)-source operating at 1480 nm.

For 2000 nm spectral range the Raman soliton generation in solid SiO_2-based LMA fibers was only reported using a passive Raman soliton approach [12]. The difference compared to the active fiber approach is that the ultrashort pulse of high energy is coupled to the undoped fiber, where it experiences nonlinear conversion. As an example, an Er-doped fiber laser emitting 1 µJ pulses with a duration of 412 fs at the wavelength of 1550 nm was coupled to a passive fiber with a core diameter of 40 µm and a cladding diameter of 200 µm to generate solitons tunable between 1580-2520 nm with a soliton duration of 100 fs and a soliton energy up to 73 nJ [12]. For a fiber with a smaller core (diameter of 35 µm) solitons with the energy of 45 nJ at 1980 nm were obtained [24]. The SiO_2 absorption limits the longest wavelength of the Raman soliton to ≈2400-2500 nm [2,12]. Longer wavelengths experience an increasing absorption due to phonons and OH-groups in the fiber. This can be mitigated by minimizing the OH-content (dry fiber) or adding GeO_x to the fiber [25], but will not completely remove the increasing absorption [26]. To be able to move to the wavelengths that are longer than 2900-3000 nm one has to use a different type of fiber, such as microstructured tellurite [27,28], fluoride [29], germanate [2,13,25,30] or chalcogenide fibers [31].

The soliton energy depends not only on the effective mode area, but also on the nonlinear refractive index of the material. This enables specialty fibers such as photonic crystal fibers (PCF) to allow significantly higher soliton energies due to the lower nonlinear refractive index n_2 of air [32]. This effect can be seen especially when comparing non-PCF LMA fibers with PCF-LMA-fibers. Here significantly higher pulse energies were reported. Horton et al. reported

Optics EXPRESS

pulse energies of 67 nJ for a pulse duration of 65 fs in a PCF-based crystal rod with an effective area of 2300 μm^2 at the pump wavelength of 1550 nm [33]. This result could be improved later to 100 nJ at a comparable pulse duration [34]. Nguyen et al., on the other hand, used a PCF-based LMA fiber with a core diameter of 20 µm and an effective area of 230 µm at 1560 nm, which generated pulses with an energy of 13 nJ and a pulse duration of 80-95 fs [35].

Summarizing, in spite of active research in the field of Raman self-frequency conversion in active fibers, to the best of our knowledge, Raman soliton generation was never reported for active Tm-doped LMA- or VLMA-type fibers. Such fibers play, however, crucial role in power scaling. The goal of this paper is to realize controlled Raman soliton generation process in Tm-doped LMA fiber, thus paving the way to energy scaling of tunable Raman solitons. To reach this overall goal, we first make a thorough investigation of the Raman self-frequency conversion in the Tm-doped all-fiber standard mode area (SMA) fiber, then study the dependence of the Raman soliton parameters on the chirp of the seed pulse, and finally realize, for the first time to our knowledge, Raman self-frequency shift inside the large mode area (LMA)-fiber amplifier pumped by 793 nm multimode diodes and seeded by a Tm femtosecond fiber laser.

2. Experimental setup

The experimental setup consists of a femtosecond Tm-fiber based seed oscillator and the two similarly-built Tm-fiber based amplifiers with different active fiber types. Those are described in the following sections.

2.1. Femtosecond fiber oscillator

The single-mode thulium-doped femtosecond oscillator had an architecture similar to the one described in [8] with the main difference being the dispersion compensating fiber added to the cavity. The dispersion control was used to manage the cavity round-trip dispersion closer to zero, which allowed to achieve femtosecond pulse generation. The laser emitted at around 1970 nm with FWHM spectral bandwidth of nearly 11 nm, as shown in Figure 1. The pulse repetition rate of the seed oscillator is 33.4 MHz, and at an average output power of 1.2 mW it corresponds to 35 pJ pulse energy. Assuming that the pulse is close to transform-limited, we estimate its duration to be 370 fs.

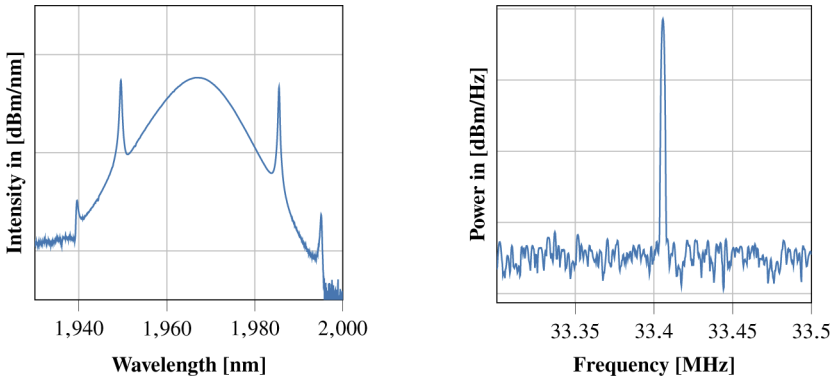

Fig. 1. Optical spectrum (left) and RF spectrum (right) of the femtosecond fiber oscillator

2.2. Tm:fiber amplifiers

Two fiber amplifiers were used in our experiments. The first amplifier is the same as described in [8]. It uses a single-mode double-clad Tm-doped active fiber with a core diameter of 10 µm

Optics EXPRESS

and the cladding of 130 µm, and thus will be further called as standard mode area (SMA) fiber amplifier. This amplifier has a fiber output: the active fiber is spliced with a standard SMF28 single-mode fiber, which allows fiber delivery of the output pulse.

The second amplifier uses the 25 µm-core double-clad large mode-area Tm-doped active fiber, and will be further called as large mode area (LMA) fiber amplifier. The amplifier is pumped in forward direction by two 105 µm core fiber-coupled multimode laser diodes emitting at 793 nm. The seed laser is combined with the pump emission through the commercial pump-signal combiner matched with amplifier active fibers. It has a free-space output: the active fiber is angle-cleaved, and the output emission is collimated using a spherical lens. The schematics of the LMA amplifier is shown in Figure 2.

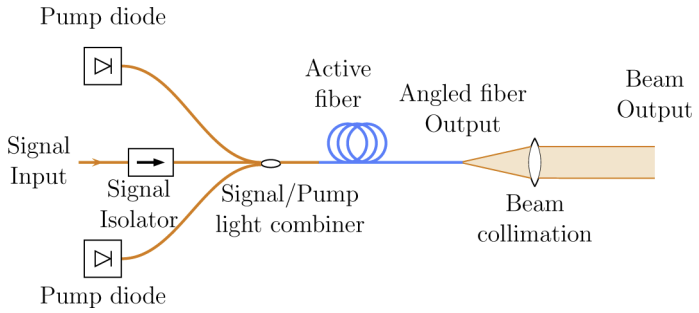

Fig. 2. Schematic of the LMA Tm:fiber amplifier

For pulse delivery from the oscillator to both amplifiers we created a fiber delivery line consisting of SMF-28 fiber and dispersion compensating fibers of different lengths. The dispersion compensating fiber in the fiber delivery line is used for chirp variation of the seed pulse, this question will be further adressed in section 3.. The polarization controller is implemented into the fiber delivery line to adjust the polarization of the seed light.

3. Experimental results

The experimental results will be described in the following order. In Section 3.1 we show how the optimization of the seed pulse chirp allows to control the position of generated Raman soliton and increase the energy transfer efficiency to Raman soliton to the values over 98 %. In Section 3.2 we make characterization of the SMA Tm:fiber amplifier with optimized seed pulse chirp, showing the limitations of the pulse energy by soliton area theorem. We also address the issues of amplification and energy loss of the Raman soliton in amplifier components depending on the soliton spectral position. Finally, in Section 3.3 we apply the same strategy to build and characterize for the first time the LMA Tm:fiber amplifier generating Raman solitons with efficiency up to 91 % and pulse energy up to 24 nJ with pulse duration of 125 fs.

3.1. Optimization of energy transfer efficiency and position of Raman soliton by adjusting the seed pulse chirp

To the best of our knowledge, the only publication indicating the influence of the seed pulse chirp on the process of Raman soliton formation in a pumped fiber amplifier [36] was based on theoretical modelling and focused on the optimization of solely the efficiency of energy transfer to Raman solitons. Our aim is to experimentally verify and extend this approach, show that the seed pulse chirp affects not only the efficiency, but also the position of Raman soliton, and thus demonstrate the way to control the process of Raman soliton formation by modification of the seed pulse chirp.

Optics EXPRESS

As it was indicated in section 2.2, in our laser system the seed oscillator is connected to the amplifier by a fiber delivery line. The delivery line consists of all the fiber elements between the oscillator output coupler and amplifier active fiber and includes fiber isolators, polarization controller, pump/signal combiner, and connectors, around 8 meters of fiber in total. While being transmitted through this fiber, the femtosecond pulse from the oscillator experiences dispersive broadening and acquires the significant chirp with a chirp parameter $C \approx -15.3$, resulting in pulse stretching from 370 fs to roughly 5 ps at the amplifier input (calculated values). Chirp parameter can be modified by implementation of the segment of ultra-high NA (0.35) fiber (UHNA) into the delivery line. UHNA-fiber has a dispersion parameter of 0.09 $ps^2\,m^{-1}$ at 1970 nm wavelength [22], roughly opposite to that of SMF-28 fiber. We experimentally vary the length of the compensating fiber from 5 m (undercompensated chirp, $C = -5.3$), to 15 m (overcompensated chirp, $C = 14.7$) with a step of 1 m while characterizing the pulse parameters at the output of the SMA fiber amplifier.

Figure 3 shows the SMA amplifier output spectra at a constant pump power of 4.7 W for different chirp values (compensating fiber lengths). No solitons are formed for 5 m and 15 m of dispersion-compensating fiber, and the only spectral component in the MOPA's output spectrum is the amplified and SPM-modified spectrum of the seed laser, and thus our laser works as a chirped pulse amplifier. For the lengths between 6 m and 14 m Raman solitons are formed and shifted to different spectral positions due to the soliton self-frequency shift effect. Thus we demonstrate that variation of the input pulse chirp allows to control the spectral position of the Raman soliton. It is clear that the configuration using 10 m of UHNA fiber (with a chirp parameter of $C \approx 4.7$) corresponds to the largest frequency shift, and thus represents the optimal compression of a seed pulse inside the amplifier.

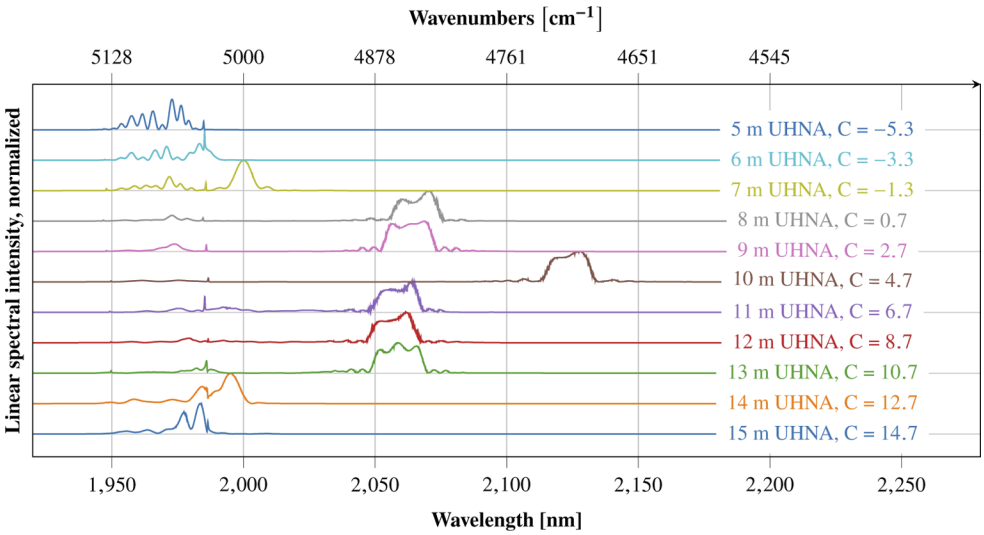

Fig. 3. Output spectra of the SMA fiber amplifier measured at a constant pump power of 4.7 W for different lengths of the dispersion-compensating fiber

One can also note the different energy distribution between Raman soliton and residuals of a seed pulse (spectral component around 1970 nm) for every spectrum given in Figure 3. While the residuals of the seed pulse are strong for up to 7 m and over 13 m of UHNA, those get weaker for the fiber lengths between 7 m and 13 m, and vanishes almost completely for 10 m of UHNA. The ratio of the soliton energy to the total energy of the output pulse can be quantified as the energy transfer efficiency to Raman soliton.

Optics EXPRESS

The dependence of the soliton generation on the length of the compensating fiber is further investigated in Figure 4 and 5. For each compensating fiber length we increased pump power until Raman soliton was spectrally shifted to the wavelength of 2050 nm, and then assessed pump power, soliton energy and energy transfer efficiency. Predictably, the lowest pump power of about 4.4 W was needed for the case of optimal compensating fiber length of 10 m, and the amplifier average output power was equal to 80 mW. For 15 m of UHNA fiber a considerably higher pump power of about 5.6 W was needed to shift the soliton to 2050 nm, and the amplifier average output power went up to 200 mW. Figure 4 shows that the intensity of the seed pulse residuals around 1970 nm strongly varies, reaching its minimum for compensating fiber length of 10 m.

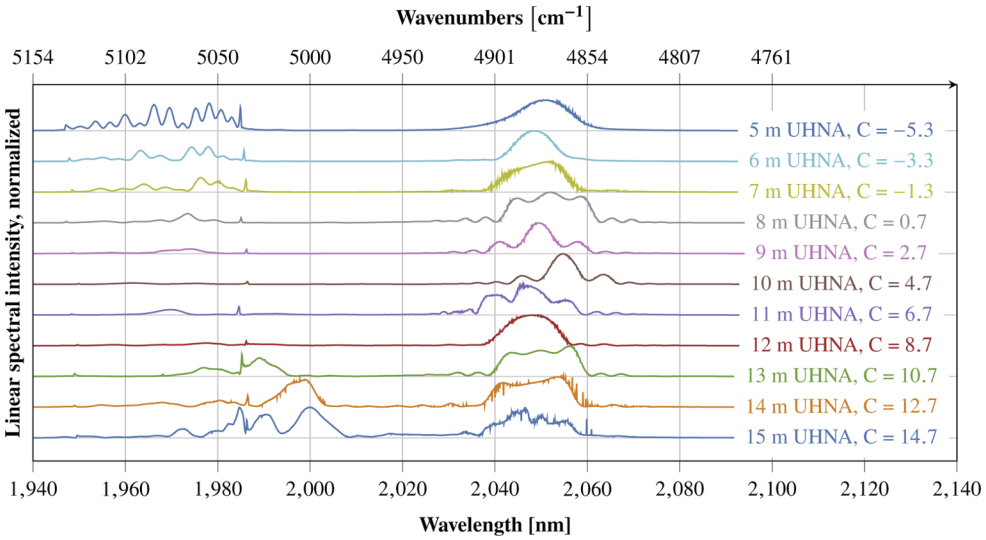

Fig. 4. Output spectra of the SMA fiber amplifier for different lengths of the dispersion-compensating fiber measured at a pump power corresponding to the first Raman soliton, located at 2050 nm

Figure 5 plots the Raman soliton energy and energy transfer efficiency vs. the length of dispersion compensating fiber and seed pulse chirp parameter. It can be seen that by optimizing the chirp we could increase the energy transfer efficiency from 40 % to over 95 %. The figure also shows that the energy of 2050 nm Raman soliton remains nearly constant (2.2-2.3 nJ) and almost independent on the dispersion compensating fiber length. The curve shows a certain trend towards increased soliton energies for the case of undercompensated chirp (C<0), and one can also note SPM-like modulations around 1970 nm for the corresponding spectra. The possible explanation to this phenomenon is that the seed pulse experience SPM-induced spectral broadening and soliton recompression in the front part of the amplifier, followed by generation of shortened and spectrally broadened Raman soliton in the tail part of the amplifier, which then can contain higher energy according to Eq. (3). However, this hypothesis can hardly be confirmed experimentally, since both the spectra and autocorrelation traces of Raman solitons emitted from SMA amplifier contain modulations, which complicate measurement of pulse duration and spectral bandwidth. Such modulations are typical for the soliton which undergoes temporal and spectral reshaping after having experienced significant loss. We assume that the source of loss is the splice between the active amplifier fiber and the output SMF28 fiber. Active fiber used in SMA amplifier is a pedestal fiber, and it is known that splicing of Thulium-doped pedestal fibers with passive fibers is challenging and might result in substantial losses [37,38].

Shortly summarizing this section, we experimentally investigated the Raman soliton generation in fiber amplifier depending on the chirp of the seed pulse. We showed that both soliton spectral

Optics EXPRESS

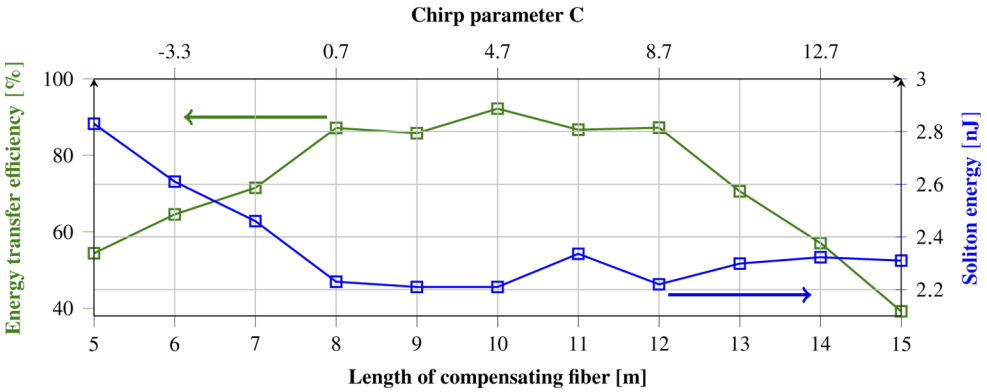

Fig. 5. Output parameters of the SMA fiber amplifier measured at a pump power corresponding to the first Raman soliton, located at 2050 nm: energy transfer efficiency to Raman soliton (green line) and corresponding soliton energy (blue line)

position and soliton energy transfer efficiency depend on the seed pulse chirp, thus demonstrating the method to control the parameters of the Raman soliton by varying the chirp of the seed pulse.

3.2. Generation of Raman solitons in the SMA amplifier

For the optimal dispersion compensating fiber length (10 m of UHNA fiber) we investigated the behavior of the Raman soliton depending on the amplifier pump power (Figure 6). At pump power of 2.95 W the output spectrum reproduces the spectrum of a seed oscillator. While pump power increases, the spectrum broadens and forms a Raman soliton, which spectrally shifts towards longer wavelengths. At 4.39 W of pump power the soliton is already at 2020 nm, and the spectral component at 1970 nm, (seed pulse residuals), vanishes almost completely, indicating very efficient energy transfer to Raman soliton. With further increase of the pump power up to 5.30 W the soliton gradually shifts to 2260 nm, while the seed pulse residuals slowly acquire energy. For the pump powers exceeding 5.57 W the Raman soliton starts losing both the energy and the "speed" of spectral shift, while the seed pulse residuals are amplified enough to form a second Raman soliton. At the 6.47 W pump power the first Raman soliton reaches the wavelength of 2320 nm and loses almost all of its energy, the second soliton is shifted to 2160 nm, and the third soliton is about to be formed from the amplified seed pulse residuals. It is important to note that the pump power could be scaled further to demonstrate the birth of more Raman solitons.

The quantitative characterization of the output pulse energy, Raman soliton energy, and efficiency of energy transfer to Raman soliton is given in Figure 7. The output pulse energy initially rises up to 2.8 nJ for the pump power of 4.6 W. This corresponds to the first Raman soliton shifted to 2100 nm. With further increase of the pump power the output pulse energy drops and reaches the minimum of 1.1 nJ for the pump power of 5.4 W. It corresponds to the first Raman soliton shifted to 2280 nm. The decreasing energy trend can be explained by the all-fiber configuration of the amplifier output – the pulse is transmitted through about 4 m of the passive SMF fiber, the absorption of which increases towards longer wavelengths. At the same time the residuals of the seed pulse are very weak (since the energy was very efficiently transferred to the first Raman soliton), and the amplification of a weak signal at 1970 nm can not compensate the energy loss by a red-shifted soliton. With further increase of the pump power above 5.5 W the first soliton slowly shifts further to 2320 nm and continuously loses energy, while the signal at 1970 nm is amplified enough to form the second Raman soliton. The contribution of amplification at 1970 nm is now dominating, and the output pulse energy increases.

Optics EXPRESS

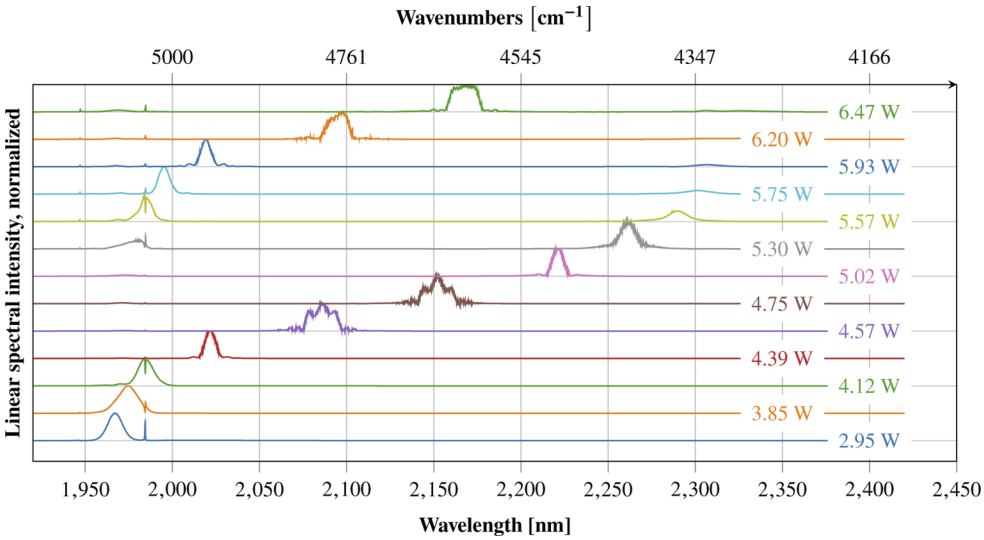

Fig. 6. Output spectra of the SMA fiber amplifier with optimal chirp compensation depending on amplifier pump power

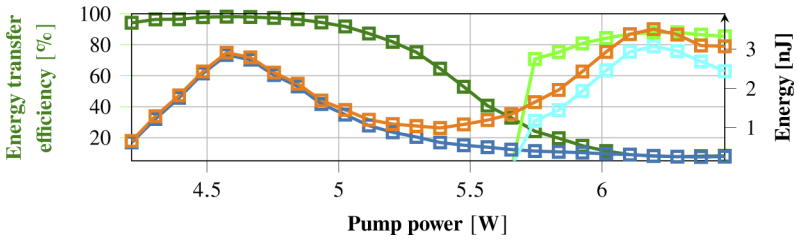

Fig. 7. Output parameters of the SMA fiber amplifier with optimal chirp compensation vs. the pump power: energy transfer efficiency to the first and the second Raman soliton (dark green and light green, respectively, left scale), output energy of the full pulse, first and second solitons (orange, dark blue, and light blue, respectively, right scale)

In addition to the total output energy Figure 7 also plots energy of first and second Raman solitons, as well as the efficiency of the energy transfer to both solitons. One can note that both the first and the second soliton reaches the energy of roughly 2.8-3.0 nJ, before losing it due to absorption in the transmitting fiber. The energy transfer efficiency to the first soliton reaches the maximum of 98.2 % at a pump power of 4.6 W, and efficiency of energy transfer to the second soliton is also very high reaching 88 % at a pump power of 6.3 W.

Different perspective opens up if one plots the energy of the first Raman soliton depending not on the pump power, but rather on its spectral position (Section 8). The figure shows that the Raman soliton experiences amplification while being frequency shifted up to 2100 nm. This unusual for a Raman soliton behavior can be explained by the fact, that the soliton is born in the pumped active Tm:fiber. Since the gain bandwidth of Tm:fiber extends to over 2050 nm [1], the soliton is being amplified within this spectral range. Being further red-shifted, soliton drifts away from the gain region towards longer wavelengths where silica begins absorbing, resulting in significant energy loss. Increase and further decrease of soliton energy results in changing the "speed" of the soliton frequency shift, as it was shown in Eq. (7) and can be clearly seen in Figure 6.

Optics EXPRESS

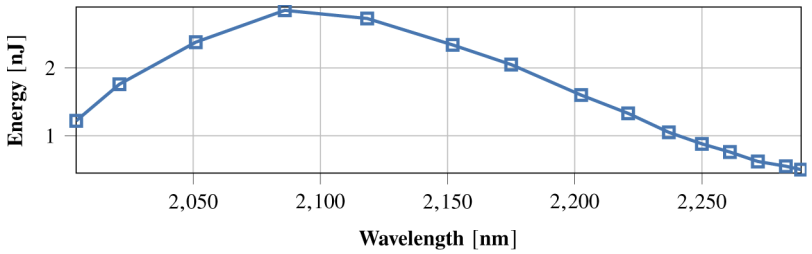

Fig. 8. Raman soliton energy in the SMA fiber amplifier with optimal chirp compensation vs. spectral position of the first Raman soliton

Spectral dependence of the soliton energy should, according to the (Eq. (3)), result in respective variations in pulse duration and spectral bandwidth of the Raman soliton. However, as already mentioned above, both spectral and autocorrelation measurements of SMA amplifier output are significantly distorted. Distortions are caused by the losses in active/passive fiber splice, and in the fiber output of the amplifier, and thus the careful numerical analysis of soliton parameters is complicated. The Raman soliton spectral bandwidth of 11 nm and pulse duration of 260 fs were estimated from the measurements done at 2050 nm (Figure 9). More detailed numerical analysis of Raman solitons pulse duration and spectral bandwidth depending on the soliton spectral position will be done below for LMA amplifier.

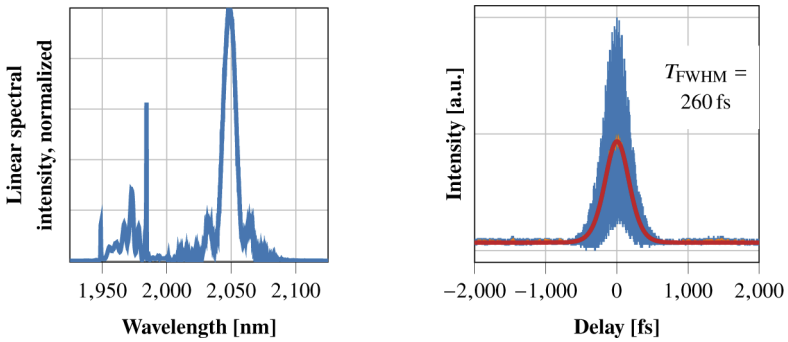

Fig. 9. Spectrum (left) and autocorrelation trace (right) of the Raman soliton located at 2050 nm emitted by SMA fiber amplifier

Shortly summarizing this section, we experimentally investigated the Raman soliton generation in optimized SMA fiber amplifier and demonstrated the soliton energy transfer efficiency of over 98 %. We showed that Raman solitons acquire energy while being shifted up to approximately 2100 nm due to amplification in thulium-doped active fiber, but then gradually loose energy while being further shifted beyond 2100 nm due to increased losses in the amplifier output fiber.

3.3. Generation of Raman solitons in the LMA amplifier

Based on the soliton behavior observed in Figure 3 and Figure 4 we applied the same strategy for soliton formation in the LMA amplifier. The fiber delivery line towards the LMA amplifier was significantly longer, and to compensate that we added additional 10 m of UHNA fiber, which, according to our estimations, brings us to the optimal compression of the seed pulse.

The development of the first Raman soliton in LMA fiber amplifier is shown in Figure 10. As for the case of SMA amplifier, one can see the transformation of the amplified seed pulse spectrum into a Raman soliton with subsequent frequency shift towards the longer wavelengths. However,

Optics EXPRESS

in this graph one can clearly see that the shift of the soliton spectral position is accompanied by increasing of the soliton spectral bandwidth.

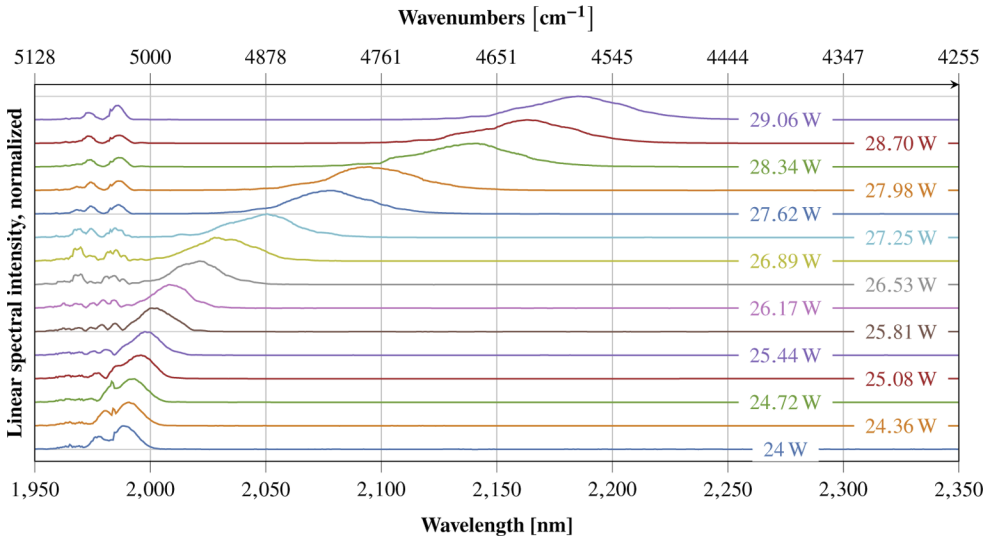

Fig. 10. Output spectra of the LMA fiber amplifier with optimal chirp compensation depending on amplifier pump power

Figure 11 shows the development of the soliton energy and efficiency of the 1st Raman soliton in the LMA fiber amplifier. Both total output pulse energy and Raman soliton energy smoothly grow following each other up to the level of about 24 nJ, which is achieved at 28.7 W of pump power. With further increase of the pump power the soliton energy remains the same, while the total output energy continues to rise reaching 45 nJ for the pump power of 34 W. Energy transfer efficiency to the first soliton reaches its maximum of 91 % at 28.7 W of pump power.

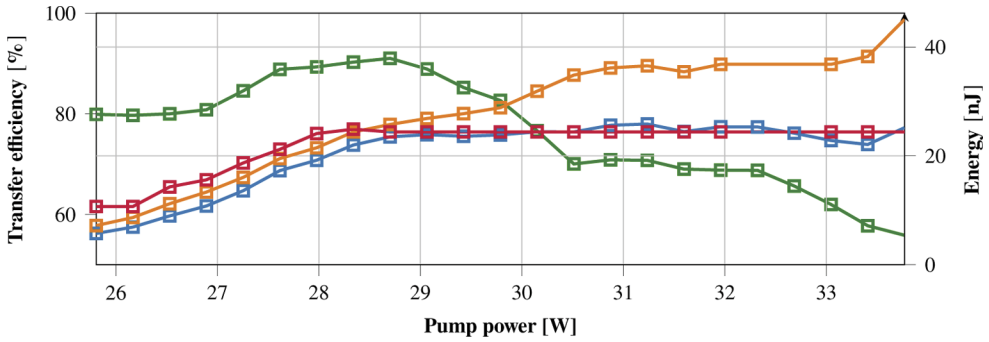

Fig. 11. Output parameters of the LMA fiber amplifier with optimal chirp compensation vs. the pump power: efficiency of energy transfer to Raman soliton (green), energy of the full pulse (orange), energy of the first Raman soliton (blue), and upper limit of the soliton energy calculated with Eq. (3) (dark red)

An important difference of LMA amplifier in comparison to the SMA amplifier is that it has a free-space output, i.e. the output pulse is coupled out of the active LMA fiber through the angled cleave, and then transmitted through the air as a collimated Gaussian beam. This fact eliminates effects observed in SMA amplifier like wavelength-dependent energy loss and spectral/temporal

Optics EXPRESS

modulations of the output soliton in a passive output fiber, and thus allows more detailed analysis of the Raman soliton development.

Figure 12 plots the Raman soliton energy (both measured and calculated using Eq. (3)), measured FWHM spectral bandwidth and pulse duration, and calculated time-bandwidth product of the Raman solitons in LMA Tm:fiber amplifier vs the spectral position of the soliton. The Raman soliton is readily developed at the wavelength of 2010 nm, with the pulse duration of 250 fs, spectral bandwidth of 19 nm, and pulse energy of 7 nJ. Similarly to the SMA amplifier, the soliton gets amplified while being frequency shifted. During the amplification both the pulse duration and the spectral bandwidth of the soliton change to accomodate for the increased energy values, following Eq. (3). The process slows down beyond 2100 nm, and beyond 2160 nm no further amplification happens. At this wavelength the soliton has pulse duration of 125 fs, spectral bandwidth of 51 nm, and pulse energy of 24 nJ. Time-bandwidth product of the generated soliton falls between 0.35 and 0.4, indicating that the pulses are close to transform limited.

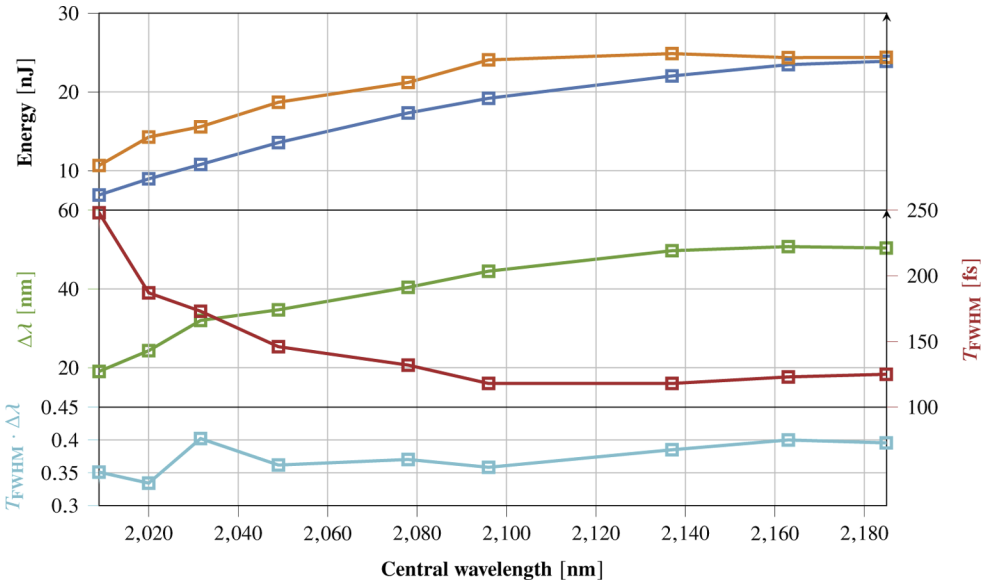

Fig. 12. Output parameters of the LMA fiber amplifier with optimal chirp compensation vs. spectral position of the first Raman soliton: soliton energy (blue), upper limit of the soliton energy calculated with Eq. (3) (orange), pulse duration (red), spectral bandwidth (green), and time-bandwidth product (light blue) of the soliton

The autocorrelation trace for the laser output at 28.7 W pump power, equivalent to Raman soliton located at 2163 nm, is shown in Figure 13. Pulse duration of 125 fs with the soliton energy of 24 nJ results in the peak power of 170 kW. Beam quality measurements (Figure 13) shows the M2 parameter of 1.7 with certain degree of astigmatism caused by the angled cleave of the fiber output.

Using the data shown in Figures 10 to 12 the validity of our experiments can be cross-checked with Eq. (6) by estimating the length of the fiber required to frequency-shift the soliton to a certain spectral position. The calculations are complicated by the fact that, as shown above, the soliton changes its duration and bandwidth while being frequency shifted, and therefore the "speed" of the frequency shift is not constant. Since Raman solitons are nearly transform-limited for the whole range of frequency shift (Figure 12), the chirp of the soliton is negligibly low, and Eq. (6) can be applied over the full range of the soliton shift. First, we make our estimations for the spectral interval where the soliton parameters are more or less constant, namely between

Optics EXPRESS

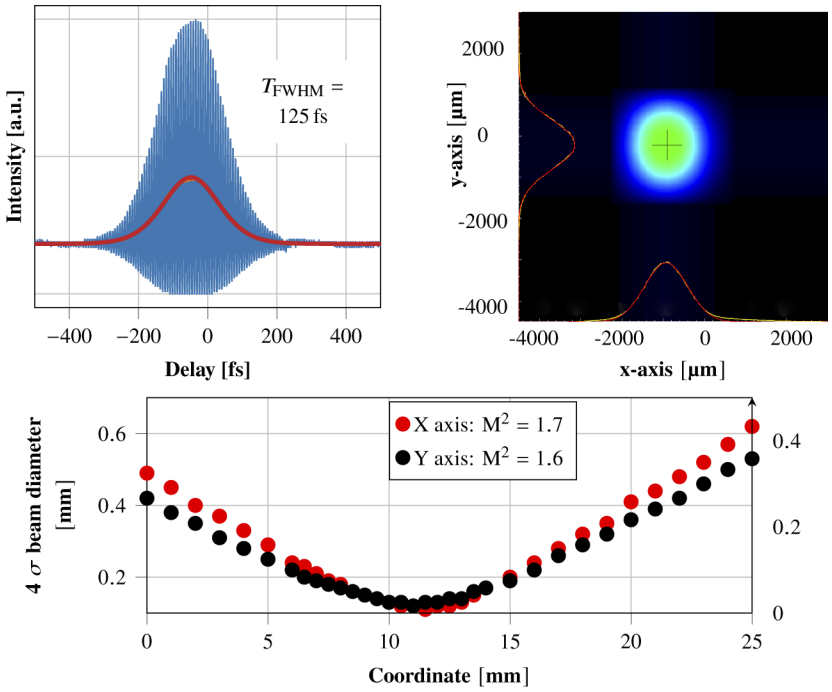

Fig. 13. Interferometric autocorrelation trace (the upper left), beam profile (upper right) and M^2-measurements (bottom) of a Raman soliton at 2163 nm generated in the LMA Tm:fiber amplifier.

2096 nm and 2137 nm. This shift corresponds to $\Delta\lambda = 41\text{nm}/\Delta\nu = 2.74\,\text{THz}$, and the dispersion of the fiber in this range is $\beta_2 = -115 \times 10^3\,\text{fs}^2\text{m}^{-1}$. According to Eq. (6):

$$z = \frac{15\Delta\nu \cdot (66.9\,\text{fs})^4}{8T_R|\beta_2|} \approx 0.30\,\text{m}, \tag{9}$$

i.e. the Raman soliton needs to travel 0.30 m through the active fiber to be shifted by 41 nm. Extrapolating this approach step-wise to the whole measured range of soliton shift, we can estimate that frequency shifting the soliton to the most long-wavelength position would require about 3.9 m of active fiber. It correlates well with the total length of the active fiber in the LMA amplifier. However, these calculations should be still considered as a rough estimation, since the frequency shift depends on the 4$^{\text{th}}$ power of the pulse duration.

When the pump power is further increased above 30 W the formation of a second Raman soliton starts (Figure 14), and the process soon becomes unstable both in terms of spectral stability and the consistence of the soliton development depending on the pump power. We attribute that to the deterioration of the polarization state of the seed light. When the pump power reaches 34 W, the third Raman soliton appears, and further increase of a pump power leads to mixing of solitons, and, finally, formation of a Raman soliton driven supercontinuum with a total pulse energy of 85 nJ for 45 W pump power. Quantitative analysis of this regime is complicated due to instabilities and fluctuations of soliton parameters.

Shortly summarizing this section, we have demonstrated Raman soliton generation in an active LMA Tm-fiber amplifier. We achieved pulses with up to 24 nJ pulse energy and 125 fs pulse duration, tunable up to 2300 nm. The energy transfer efficiency to Raman soliton reached 91 %.

Optics EXPRESS

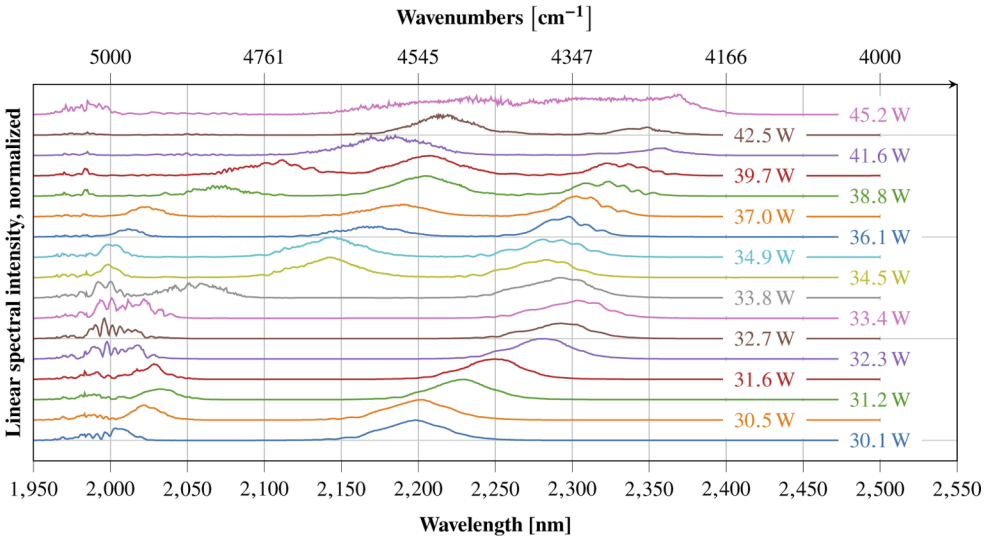

Fig. 14. Output spectra of the LMA fiber amplifier with optimal chirp compensation depending on amplifier pump power: second and third Raman soliton

4. Conclusion and outlook

We investigated the Raman soliton generation in diode-pumped Tm-doped fiber amplifiers based on single-mode double-clad and large-mode-area fibers seeded with femtosecond pulses from Tm-doped fiber oscillator. Several important results and conclusions could be drawn from this investigation that pave the way towards future energy scaling of Raman shifted solitons:

- We demonstrated for the first time to our knowledge the Raman soliton generation inside the Tm:doped LMA fiber amplifier tunable up to 2300 nm, reaching the pulse energy of 24 nJ with a pulse duration of 125 fs and a peak power of 170 kW.
- We demonstrated for the first time to our knowledge the way to control both the spectral position and the energy transfer efficiency to a Raman soliton generated in a fiber amplifier by varying the chirp of the seed pulse. We could achieve over 98 % energy transfer efficiency to the Raman soliton in the SMA amplifier, and over 91 % for the LMA-amplifier.
- We analyzed dynamics of the Raman soliton formation in the LMA amplifier, showing that Raman solitons undergo amplification in an amplifier active fiber if their spectral position is within the gain range of Tm, and that such amplification is accompanied by spectral broadening and temporal shortening of the soliton. Beyond the Tm gain wavelength range Raman shifting continues, but is not associated with further spectral broadening/temporal shortening.
- The long wavelength edge of the Raman pulse tuning is limited by the presence of OH-complexes in silica glass and can be counteracted by a proper choice of fiber material.
- We confirmed the validity of the correlation between the frequency shift, the pulse duration and the pulse energy (as demonstrated in Eqs. (6) and (7))
- Finally, we experimentally confirmed that the energy of the generated Raman soliton is limited by the soliton area theorem.

Optics EXPRESS

The work has thus demonstrated the principal possibility of Raman self-frequency shift in active LMA fibers. It has also shed light on the mechanisms of Raman self-frequency shift in active ion-doped fiber amplifiers, establishing the limits of the pulse energy increase in silica LMA fibers. Further energy scaling and Raman tuning should be possible via using, for example, larger solid-core LMA amplifiers or crystalline waveguides. However, even in the present form the developed tunable Raman MOPA system is useful in many spectroscopic and remote-sensing applications requiring broad electronic tunability and high sensitivity.

Funding. Norges Forskningsråd (219686, 255003, 303347).

Acknowledgements. The authors would like to thank Lars Holmen (Forsvarets Forskningsinstitut, Oslo) and Till Walbaum (Fraunhofer IOF, Jena) for the help with optimizing the LMA-fiber based amplifier. We also would like to thank Evgeni Sorokin (TU Wien, Vienna) for fruitful discussions about the optimization and improving the laser systems. The work was supported by the Research Council of Norway projects 219686, 255003 (KerfLessSi), 303347 (UNLOCK) and ATLA Lasers AS.

Disclosures. The authors declare no conflicts of interest.

Data availability. Data underlying the results presented in this paper are not publicly available at this time, but may be obtained from the authors upon reasonable request.

References

1. Z. Li, A. M. Heidt, N. Simakov, Y. Jung, J. M. O. Daniel, S. U. Alam, and D. J. Richardson, "Diode-pumped wideband thulium-doped fiber amplifiers for optical communications in the 1800-2 050nmwindow," Opt. Express **21**(22), 26450 (2013).
2. V. V. Dvoyrin and I. T. Sorokina, "Optical fiber amplifier," International (PCT) Patent PCT/EP2014/059252 (WO2014/177724) (3 May 2013).
3. V. V. Dvoyrin, D. Klimentov, and I. T. Sorokina, "3 W Raman Soliton Tunable between 2-2 2μmin Tm-Doped Fiber MOPA," in *Advanced Solid-State Lasers Congress*, (OSA, Washington, D.C., 2013), p. MTh1C.2.
4. I. T. Sorokina, V. V. Dvoyrin, N. Tolstik, and E. Sorokin, "Mid-IR Ultrashort Pulsed Fiber-Based Lasers," IEEE J. Sel. Top. Quantum Electron. **20**(5), 99–110 (2014).
5. G. Imeshev and M. E. Fermann, "230-kW peak power femtosecond pulses from a high power tunable source based on amplification in Tm-doped fiber," Opt. Express **13**(19), 7424 (2005).
6. S. Kivisto, T. Hakulinen, M. Guina, and O. G. Okhotnikov, "Tunable Raman Soliton Source Using Mode-Locked Tm–Ho Fiber Laser," IEEE Photonics Technol. Lett. **19**(12), 934–936 (2007).
7. V. V. Dvoyrin and I. T. Sorokina, "6.8 W all-fiber supercontinuum source at 1.9-2 5μm," Laser Phys. Lett. **11**(8), 085108 (2014).
8. D. Klimentov, N. Tolstik, V. V. Dvoyrin, R. Richter, and I. T. Sorokina, "Flat-Top Supercontinuum and Tunable Femtosecond Fiber Laser Sources at 1.9-2 5μm," J. Lightwave Technol. **34**(21), 4847–4855 (2016).
9. P. Wang, H. Shi, F. Tan, and P. Wang, "Enhanced tunable Raman soliton source between 1.9 and 2.36 μm in a Tm-doped fiber amplifier," Opt. Express **25**(14), 16643 (2017).
10. V. V. Dvoyrin and S. K. Turitsyn, "Generation of high-energy soliton-like pulses in 1.9–2.5 μ m spectral domain," Journal of Physics: Photonics **2**(4), 044005 (2020).
11. F. Liu, J. Li, H. Luo, Q. Wu, X. Wu, F. Ouellette, and Y. Liu, "Study on soliton self-frequency shift in a Tm-doped fiber amplifier seeded by a Kelly-sideband-suppressed conventional soliton," Opt. Express **29**(5), 6553 (2021).
12. B. Li, M. Wang, K. Charan, M.-j. Li, and C. Xu, "Investigation of the long wavelength limit of soliton self-frequency shift in a silica fiber," Opt. Express **26**(15), 19637 (2018).
13. Y. Li, T. Du, B. Xu, H. Xu, Z. Cai, V. M. Mashinsky, and Z. Luo, "Compact all-fiber 2.1-2 7μmtunable Raman soliton source based on germania-core fiber," Opt. Express **27**(20), 28544 (2019).
14. D. Strickland and G. Mourou, "Compression of amplified chirped optical pulses," Opt. Commun. **56**(3), 219–221 (1985).
15. N. G. Broderick, H. L. Offerhaus, D. J. Richardson, and R. A. Sammut, "Power scaling in passively mode-locked large-mode area fiber lasers," IEEE Photonics Technol. Lett. **10**(12), 1718–1720 (1998).
16. A. Galvanauskas, "Mode-scalable fiber-based chirped pulse amplification systems," IEEE J. Sel. Top. Quantum Electron. **7**(4), 504–517 (2001).
17. W. Jin, W. Xu, Z. Chen, Y. Xu, B. Yu, H. Cui, and S. Liu, "Effect of frequency chirping on supercontinuum generation in dispersion flatted and dispersion decreasing fiber," Phys. Lett. Sect. A: Gen. At. Solid State Phys. **333**(5-6), 415–419 (2004).
18. J. Wen, H. Liu, N. Huang, Q. Sun, and W. Zhao, "Influence of the initial chirp on the supercontinuum generation in silicon-on-insulator waveguide," Appl. Phys. B: Lasers Opt. **104**(4), 867–871 (2011).
19. G. P. Agrawal, "Nonlinear Fiber Optics," in *Nonlinear Science at the Dawn of the 21st Century*, P. L. Christiansen, M. P. Sørensen, and A. C. Scott, eds. (Springer Berlin Heidelberg, Berlin, Heidelberg, 2000), pp. 195–211.
20. D. Marcuse, "Pulse distortion in single-mode fibers 3: Chirped pulses," Appl. Opt. **20**(20), 3573 (1981).

Optics EXPRESS

21. J. P. Gordon, "Theory of the soliton self-frequency shift," Opt. Lett. **11**(10), 662 (1986).
22. P. Ciacka, A. Rampur, A. Heidt, T. Feurer, and M. Klimczak, "Dispersion measurement of ultra-high numerical aperture fibers covering thulium, holmium, and erbium emission wavelengths," J. Opt. Soc. Am. B **35**(6), 1301 (2018).
23. J. W. Nicholson, A. Desantolo, W. Kaenders, and A. Zach, "Self-frequency-shifted solitons in a polarization-maintaining, very-large-mode area, Er-doped fiber amplifier," Opt. Express **24**(20), 23396 (2016).
24. Ke Wang, N. G. Horton, K. Charan, and C. Xu, "Advanced Fiber Soliton Sources for Nonlinear Deep Tissue Imaging in Biophotonics," IEEE J. Sel. Top. Quantum Electron. **20**(2), 50–60 (2014).
25. V. V. Dvoyrin, I. T. Sorokina, V. M. Mashinsky, L. D. Ischakova, E. M. Dianov, V. L. Kalashnikov, M. V. Yashkov, V. F. Khopin, and A. N. Guryanov, "Tm^{3+}-doped CW fiber laser based on a highly GeO_2-doped dispersion-shifted fiber," Opt. Express **19**(9), 7992 (2011).
26. O. Humbach, H. Fabian, U. Grzesik, U. Haken, and W. Heitmann, "Analysis of OH absorption bands in synthetic silica," J. Non-Cryst. Solids **203**, 19–26 (1996).
27. X. Yan, G. Qin, M. Liao, T. Suzuki, and Y. Ohishi, "Enhanced soliton self-frequency shift in tellurite microstructured fiber," in *16th Opto-Electronics and Communications Conference, OECC 2011* pp. 49–50 (2011).
28. Z. Li, N. Li, C. Yao, F. Wang, Z. Jia, F. Wang, G. Qin, Y. Ohishi, and W. Qin, "Tunable mid-infrared Raman soliton generation from 1.96 to 2.82 μm in an all-solid fluorotellurite fiber," AIP Adv. **8**(11), 115001 (2018).
29. Y. Tang, L. G. Wright, K. Charan, T. Wang, C. Xu, and F. W. Wise, "Generation of intense 100 fs solitons tunable from 2 to 4.3 μm in fluoride fiber," Optica **3**(9), 948 (2016).
30. V. V. Dvoyrin and I. T. Sorokina, "All-fiber optical supercontinuum sources in 1.7-3 2μmrange," in *Fiber Lasers XI: Technology, Systems, and Applications*, vol. 8961 S. Ramachandran, ed. (2014), p. 89611C.
31. F. Wang, Q. Li, Z. Kang, C. F. Wu, D. Ding, G. S. Qin, Z. Y. Yang, and Y. Ohishi, "Numerical demonstration of widely tunable femtosecond soliton generation in chalcogenide microstructured fibers," Laser Phys. Lett. **16**(10), 105402 (2019).
32. J. H. Lee, J. van Howe, C. Xu, and X. Liu, "Soliton Self-Frequency Shift: Experimental Demonstrations and Applications," IEEE J. Sel. Top. Quantum Electron. **14**(3), 713–723 (2008).
33. N. G. Horton, K. Wang, D. Kobat, C. G. Clark, F. W. Wise, C. B. Schaffer, and C. Xu, "In vivo three-photon microscopy of subcortical structures within an intact mouse brain," Nat. Photonics **7**(3), 205–209 (2013).
34. N. G. Horton and C. Xu, "Dispersion compensation in three-photon fluorescence microscopy at 1, 700 nm," Biomed. Opt. Express **6**(4), 1392 (2015).
35. T. N. Nguyen, K. Kieu, D. Churin, T. Ota, M. Miyawaki, and N. Peyghambarian, "High Power Soliton Self-Frequency Shift With Improved Flatness Ranging From 1.6 to 1.78 μm," IEEE Photonics Technol. Lett. **25**(19), 1893–1896 (2013).
36. J. Luo, B. Sun, J. Ji, E. L. Tan, Y. Zhang, and X. Yu, "High-efficiency femtosecond Raman soliton generation with a tunable wavelength beyond 2 μm," Opt. Lett. **42**(8), 1568 (2017).
37. C. Jollivet, K. Farley, M. Conroy, H. Dabhi, J. Edgecumbe, A. Carter, and K. Tankala, "Design optimization of Tm-doped large-mode area fibers for power scaling of 2 μm lasers and amplifiers," in *Fiber Lasers XIV: Technology and Systems*, vol. 10083, C. A. Robin and I. Hartl, eds. (2017), p. 100830I.
38. B. M. Anderson, J. Soloman, and A. Flores, "1.1 kW, beam combinable thulium doped all-fiber amplifier," in *Fiber Lasers XVIII: Technology and Systems*, M. N. Zervas and C. Jauregui-Misas, eds. (SPIE, 2021), March, p. 7.